Research paper

Discoidin domain receptor 1 activation links extracellular matrix to podocyte lipotoxicity in Alport syndrome

Jin-Ju Kim[a],[†],[*], Judith M. David[a],[†], Sydney S. Wilbon[a], Javier V. Santos[a], Devang M. Patel[b], Anis Ahmad[c], Alla Mitrofanova[a],[d], Xiaochen Liu[a], Shamroop K. Mallela[a], Gloria M. Ducasa[a], Mengyuan Ge[a], Alexis J. Sloan[a], Hassan Al-Ali[a], Marcia Boulina[e], Armando J. Mendez[e], Gabriel N. Contreras[a], Marco Prunotto[f],[i], Anjum Sohail[g], Rafael Fridman[g], Jeffrey H. Miner[h], Sandra Merscher[a], Alessia Fornoni[a],[*]

[a] Katz Family Division of Nephrology and Hypertension, Drug Discovery center, Department of Medicine, University of Miami Miller School of Medicine, 1580 NW 10th Ave, Miami, FL 33136, United States
[b] Department of Diabetes, Central Clinical School, Monash University, Melbourne, Australia
[c] Department of Radiation Oncology, University of Miami, FL 33136, United States
[d] Department of Surgery, University of Miami Miller School of Medicine, Miami, FL 33136, United States
[e] Diabetes Research Institute, University of Miami Miller School of Medicine, Miami, FL 33136, United States
[f] Roche Pharma Research and Early Development, Roche Innovation Center, Basel, Switzerland
[g] Department of Pathology, Wayne State University School of Medicine, Detroit, Michigan 48201, United States
[h] Division of Nephrology, Department of Medicine, Washington University School of Medicine, St. Louis, Missouri 63110, United States
[i] School of Pharmaceutical Sciences, University of Geneva, Geneva, Switzerland

ARTICLE INFO

ABSTRACT

Background: Discoidin domain receptor 1 (DDR1) is a receptor tyrosine kinase that is activated by collagens that is involved in the pathogenesis of fibrotic disorders. Interestingly, *de novo* production of the collagen type I (Col I) has been observed in Col4a3 knockout mice, a mouse model of Alport Syndrome (AS mice). Deletion of the DDR1 in AS mice was shown to improve survival and renal function. However, the mechanisms driving DDR1-dependent fibrosis remain largely unknown.
Methods: Podocyte pDDR1 levels, Collagen and cluster of differentiation 36 (CD36) expression was analyzed by Real-time PCR and Western blot. Lipid droplet accumulation and content was determined using Bodipy staining and enzymatic analysis. CD36 and DDR1 interaction was determined by co-immunoprecipitation. Creatinine, BUN, albuminuria, lipid content, and histological and morphological assessment of kidneys harvested from AS mice treated with Ezetimibe and/or Ramipril or vehicle was performed.
Findings: We demonstrate that Col I-mediated DDR1 activation induces CD36-mediated podocyte lipotoxic injury. We show that Ezetimibe interferes with the CD36/DDR1 interaction *in vitro* and prevents lipotoxicity in AS mice thus preserving renal function similarly to ramipril.
Interpretation: Our study suggests that Col I/DDR1-mediated lipotoxicity contributes to renal failure in AS and that targeting this pathway may represent a new therapeutic strategy for patients with AS and with chronic kidney diseases (CKD) associated with Col4 mutations.
Funding: This study is supported by the NIH grants R01DK117599, R01DK104753, R01CA227493, U54DK083912, UM1DK100846, U01DK116101, UL1TR000460 (Miami Clinical Translational Science Institute, National Center for Advancing Translational Sciences and the National Institute on Minority Health and Health Disparities), F32DK115109, Hoffmann-La Roche and Alport Syndrome Foundation.

1. Introduction

Chronic kidney disease is a major healthcare problem that affects several hundred million people worldwide and is the 9th cause of death in United States [1,2]. About 25% of patients report a family history of CKD, which has led to the identification of several mutations in podocyte

* Corresponding authors.
E-mail addresses: jjkim@med.miami.edu (J.-J. Kim), afornoni@med.miami.edu (A. Fornoni).
† These authors contributed equally to the work

Research in context

Evidence before this study

Collagen (Col) type IV mutations are pathogenic mutations associated with chronic kidney disease (CKD). In patients with Alport Syndrome (AS), Col4A3, Col4A4 or Col4A5 mutations disturb the proper formation of basement membranes in kidney (GBM), eye, and inner ear. Disruption of the integrity of the GBM results in proteinuria, progressive renal fibrosis and failure during adolescence or early adulthood. However, there is no specific treatment currently available beyond ACE inhibitors.

Added value of this study

In this study, we unveil a novel mechanism by which abnormal glomerular basement membrane (GBM) mediated aberrant DDR1 activation induces podocyte lipotoxicity, thus contributing to the progression of AS. We demonstrate that Ezetimibe, an FDA-approved drug which lowers lipid absorption, improves renal function and lipid metabolism in a mouse model of AS.

Implications of all the available evidence

This study could provide an important breakthrough in the search for repurposed treatment strategies for patients with AS.

genes [3-6] in early onset and familial cases. With the wider utilization of genetic testing in patients affected by other glomerular diseases, such as familial steroid-resistant focal segmental glomerulosclerosis (FSGS), Col IV mutations were found to be the second most pathogenic mutation in patients with CKD [7,8,9], suggesting that the prevalence of Alport Syndrome (AS) has been largely underestimated. Alport Syndrome (AS), a rare genetic condition that leads to progressive kidney disease, is characterized by mutations in the genes coding for collagen type IV (Col4A3, Col4A4, Col4A5) [10-12].Mutations in the $\alpha3$, $\alpha4$, or $\alpha5$ chains of collagen IV encoding genes disturb the normal formation of the capillary basement membranes in the kidney [11], eye [13], and inner ear [14]. Disruption of the integrity of the glomerular filtration barrier results in hematuria and proteinuria followed by progressive glomerular and tubulointerstitial fibrosis and renal failure [15]. Patients with AS develop end stage renal disease (ESRD) during adolescence or early adulthood. Yet, no specific treatment is currently available for patients with AS, and Ramipril (RM) is the only standard-of-care based on retrospective studies [16] in a recent phase two study of adolescents affected by AS [17]. Furthermore, given the high prevalence of collagen genes mutations in CKD, treatment strategies for AS may result more broadly in novel therapeutic option for a large portion of patients with CKD.

Renal failure associated with AS highlights the importance of the glomerular basement membrane (GBM) composition in the maintenance of the glomerular filtration barrier (GFB). In vivo, Col IV exists in three isoforms called $\alpha1\alpha1\alpha2$, $\alpha3\alpha4\alpha5$, and $\alpha5\alpha5\alpha6$ [18,19]. During normal kidney development, the immature $\alpha1\alpha1\alpha2$ isoform of Col IV is replaced by the $\alpha3\alpha4\alpha5$, the main component of the mature GBM [20-22]. However, this developmental switch is arrested in AS due to mutations in one of the three genes (COL4A3, COL4A4, or COL4A5) that encode the $\alpha3$, $\alpha4$, and $\alpha5$ chains of Col IV [20,23]. In patients with AS [24] and in Col4a3KO mice, a mouse model for AS, the $\alpha1\alpha1\alpha2$ isomer persists in the GBM in the absence of the $\alpha3\alpha4\alpha5$ network. This aberrant collagen network in the GBM is insufficient to preserve kidney function and is associated with the development of hematuria, proteinuria and renal failure early in life[25,26]. Furthermore, de novo production of Collagen type I $\alpha1$ (Col1A1) and $\alpha2$ chains (Col1A2) in the GBM at both transcriptional and translational level, has been observed in Col4a3KO mice and in AS patients [27-29].

Besides its reliance on GBM composition, the integrity of the GFB also depends on cell-cell and cell-matrix adhesions, predominantly of podocytes [30]. Podocytes are highly specialized glomerular epithelial cells that line the urinary space of the GBM [31]. Podocytes adhere to the GBM via adhesion receptors such as integrins, syndecans, and dystroglycans [32]. Therefore, it is feasible that podocyte injury in AS results from an impairment in podocyte-GMB cross talk [32,33].

Before the discovery of Discoidin Domain Receptor 1 (DDR1), integrins were considered the only class of cell surface receptors that could transmit intracellular signals by binding extracellular matrix (ECM) proteins [34,35]. DDR1 is a tyrosine kinase receptor expressed in 5 isoforms, DDR1a-e. DDR1 is expressed mostly by epithelial cells but is also expressed by mesenchymal cells. DDR1 is activated by fibrillar and non-fibrillar collagens [36-38]. The discoidin domain of the DDR1 contains the collagen-binding region and is responsible for mediating DDR1 and collagen interaction [39]. Upon the collagen I binding, DDR1 undergoes tyrosine autophosphorylation, and the phosphorylation levels persist for days, with no apparent means for signal attenuation [37,40]. Activation of DDR1 by collagens has been shown to promote fibrosis and inflammation, generating a positive feedback loop that perpetuates DDR1 activation [37,41]. Interestingly, deletion of DDR1 in Col4a3KO mice was shown to improve renal function and survival [12], and we recently reported that treatment of Col4a3KO mice with a selective DDR1 inhibitor improves renal function and fibrosis [29]. However, the mechanism(s) by which DDR1 activation by aberrant Col I production contributes to podocyte injury in AS remains elusive.

We and others have shown dysregulated renal lipid metabolism in Col4a3KO mice [42,43], similar to what was previously described in glomeruli in clinical and experimental FSGS and diabetic kidney disease (DKD) [42,44-47]. While we reported that dysregulated cholesterol efflux is a key determinant of podocyte injury in several glomerular disorders, including AS [42,44], others described the role of cholesterol influx [43] and cluster of differentiation 36 (CD36)-dependent free fatty acid (FFA) uptake in podocyte injury [48, 49]. CD36 is a protein involved in FFA uptake, cholesterol absorption and the activation of inflammatory pathways [50-52]. Clinical and experimental studies suggest that disturbed FFA metabolism in podocytes plays a critical pathogenic role in obesity-related glomerulopathy and DKD [48,53].

Our study demonstrates enhanced DDR1b/c activation in AS and in podocytes exposed to Col I and a novel mechanism in which DDR1b/c activation induces increased podocyte FFA uptake, leading to podocyte damage. These findings uncover a novel link between ECM-initiated signaling and lipid metabolism in podocytes. In vivo, we used Col4a3 knockout mice (AS mice) as a mouse model for CKD to demonstrate that the inhibition of CD36-dependent FFA uptake with the clinically available compound, Ezetimibe (EZ) [54-56], protects from renal failure in Col4a3KO mice similarly to RM.

2. Methods

2.1. Study approval and design

EZ was orally administered at a concentration of 5 mg/kg BW, RM was added to the drinking water at a concentration that would lead to a daily RM uptake of 10 mg/kg BW. All mice were sacrificed at 8 weeks of age. The following four groups of mice were analyzed: WT, Col4a3 KO + EZ, Col4a3 KO + RM, Col4a3 KO + EZ + RM. The primary objective of this study was to determine novel mechanism by which collagen - mediated DDR1 activation causes podocyte lipotoxicity leading to the progression of AS. To investigate this mechanism, we measured the cellular LD content and the levels of FFA uptake in collagen treated podocytes. We further used DDR1 (wild type, self-activating (N211Q), and kinase dead (K655A)) overexpressing human podocyte cell lines to confirm the mechanism. In vivo studies were performed and the lipid content and renal function in Col4a3 KO mice (129-Col4a3^{tm1Dec}/J, stock number 002,908, Jackson

Laboratories) were determined. Two groups of mice ($n = 8-10$ per group; wildtype and Col4a3 KO) were analyzed at 8 weeks of age. We also investigated if EZ, an FDA-approved drug prescribed to lower lipid absorption, or a combination therapy of EZ and RM can improve lipid metabolism and renal function in Col4a3 KO mice. Six groups of mice ($n = 5-10$ per group) were examined (WT, WT+EZ, Col4a3 KO, Col4a3 KO+EZ, Col4a3 KO+RM, and Col4a3 KO+EZ+RM). Mice were treated starting at four-weeks of age and sacrificed at eight-weeks of age. All animal studies were approved by the Institutional Animal Care and Use Committee (IACUC) at the University of Miami. Minimal group sizes for *in vitro* and *in vivo* studies were determined via power calculation using the DSS Researcher's Toolkit with an α of 0.05. Animals were grouped unblinded, but randomized, and investigators were blinded for the quantification experiments. GraphPad Prism Outlier calculator software (https://www.graphpad.com/quickcalcs/Grubbs1.cfm) was used to indicate outliers in each set of data obtained for *in vitro* and *in vivo* experiments. Significant outliers were excluded from further statistical analysis. All experiments were performed at least twice. Additional information about Methods can be found in the Supplemental Material.

2.2. Ethics statements

All animal studies were performed according to protocols approved by the Institutional Animal Care and Use Committee (IACUC) at the University of Miami.

2.3. Establishment of conditionally immortalized mouse podocyte cell lines isolated from WT and Col4a3 KO mice

To establish immortalized mouse podocyte cell lines, Col4a3 +/- mice were bred with the Immorto-mice carrying a temperature-sensitive T-antigen transgene (SV40+/-) [57] purchased from Charles River (CBA/CaxC57BL/10-H-2K^b-tsA58) to generate double heterozygous littermates. Double heterozygous littermates were then crossed. SV40Tg/+; Col4a3-/- (immorto-Col4a3 KO) and SV40Tg/Tg +/-; Col4a3+/+ (immorto-wildtype) were identified by genotyping PCR and glomeruli were isolated. Podocytes were grown out from the isolated glomeruli and cultured, as previously described [58]. Immortalized mouse podocyte cell lines were confirmed by Western blot analysis of podocyte markers after 12 days of differentiation at 37 °C.

2.4. Establishment DDR1b-expressing podocytes

Stable human podocyte cell lines expressing GFP-tagged DDR1b mutants, wild type, and empty (EV) vectors were developed by lentiviral infection. We used the following DDR1b mutants: DDR1b N211Q and DDR1b K655A. Mutations at the N211 site of DDR1 located within the discoidin domain result in collagen-independent autoactivation of the receptor [59]. Here, we refer to the N211A mutant of DDR1b as self-activating (SA/DDR1b). Mutations at the conserved K655 site within the kinase domain of DDR1b generate a mutant that is catalytically inactive and thus is not phosphorylated in response to collagen [60]. We refer to this mutant as kinase dead (KD/DDR1b). We purchased these 4 lentiviral plasmids (pLV-Puro-CMV-hDDR1b: EGFP (DDR1b WT), pLV-Puro-CMV-hDDR1b (N211Q): EGFP (DDR1b SA), pLV-Puro-CMV-hDDR1b (K655A): EGFP (DDR1b KD), and pLV-Puro-CMV: EGFP (EV) from Vector Builder. After lentiviral infection, clones were obtained by limited dilution and expanded under puromycin selection followed by cell sorting. The sorted cells were confirmed by Western blot analysis for pDDR1, DDR1 and GFP. The engineered human podocyte cell lines grown at 33 °C were then transferred to 37 °C to induce differentiation for 12 days. Western blot analysis for synaptopodin (Santacruz, sc-21,537) in these cell lines confirmed that DDR1b overexpression did not affect podocyte differentiation at 37 °C.

2.5. Podocyte cell culture

Human podocytes were cultured at 33 °C under permissive conditions in RPMI culture medium containing 10% FBS and 1% penicillin/streptomycin and 0.01 mg/ml recombinant human insulin, 0.0055 mg/ml human transferrin (substantially iron-free), and 0.005 μg/ml sodium selenite [61]. Human podocytes were then thermoshifted and differentiated for 14 days at 37 °C in RPMI medium 10% FBS and 1% penicillin/streptomycin. On day 12 of differentiation, DDR1-expressing and control human podocytes were serum-starved for 24 h, followed by treatment with Col I (Corning, 100 μg/mL, 18 hrs). The cells were then lysed with cell lysis buffer (Cell Signaling) and examined for DDR1b activation by Western Blot analysis. Differentiated DDR1b-expressing podocytes were used in various assays as described below.

2.6. Immunoprecipitation and Western blot analysis

Kidney cortex was homogenized in cell lysis buffer (Cell Signaling) containing Phosphatase Inhibitor Cocktail Complete EDTA free (Roche Applied Sciences, Switzerland), and PMSF 0.1 M (Sigma, St Louis, MO). Homogenized tissues were centrifuged at 2000 g for 10 min at 4 °C. Supernatants were collected. Human podocyte cell lysates were prepared using the same lysis buffer described above and protein concentrations of tissue and cell lysates were estimated with the BCA protein assay. Then 1.5 mg of protein were mixed with anti-human antibody DDR1 (R&D) for 1 h at 4 °C with continuous agitation. The reaction mixtures were incubated with 50% slurry of protein G-sepharose (GE Healthcare, Sweden) at 4 °C for 2 h and centrifuged at 4000 rpm for 30 s. The pellets were resuspended in sample buffer solution NuPAGE 4x (Life Technologies) and NuPAGE sample reducing agent 10x containing 500 mM DTT (Life Technologies), boiled for 5 min at 95 °C, and centrifuged at 10,000 rpm for 15 s. For Western blot, protein amount of 15 μL for phospho DDR1 detection and 5 μL for DDR1 detection were loaded for SDS-PAGE on 4-20% gels and transferred to nitrocellulose membranes. The duplicate blots were probed with rabbit anti-human C-terminus DDR1 1:5000 (C-20, Santa Cruz, sc-532) at 4 °C overnight or rabbit anti-phospho DDR1 1:1000 (Y513, Cell Signaling, #14,531) followed by corresponding secondary antibody. Detection was carried out using ECL Western blotting detection reagents (GE Healthcare, UK). For collagen detection, kidney tissue and human podocyte lysates were prepared as described above. Forty μg of total protein was loaded, and the blot was probed with rabbit anti-collagen I 1:1000 (Aviva System, OAAB10798) that detects c-terminus of Col I, at 4 °C overnight followed by corresponding secondary antibody.

2.7. Quantitative real-time PCR

RNA was extracted from isolated glomeruli using the RNeasy Mini Kit (Qiagen). Reverse transcription was performed using qScript cDNA SuperMix (Quanta) according to the manufacturer's protocols. Quantitative real-time PCR (RT-PCR) was performed using the StepOnePlus system (Applied Biosystems) with PerfeCTA SYBR Green FastMix (Quanta).

2.8. Isolation of plasma membranes

Cells were collected in homogenization media (15 mM KCl, 1.5 mM MgCl$_2$, 10 mM HEPES, 1 mM DTT) and incubated on ice for 5 min. Cell pellets were homogenized 5 times using insulin syringes and incubated with 2.5 M sucrose solution (250 nM final concentration). Cell pellets were submitted to several centrifugation steps: to separate nuclear fraction (1,000xg, 5 min, 4 °C); to separate mitochondrial and endoplasmic reticulum fraction (10,000xg, 15 min, 4 °C); to separate plasma membrane fraction and cytosolic fraction

(100,000x*g*, 1 h, 4 °C). Resulting membrane pellets were collected and resuspended in 50 μL of homogenization media followed by Western blot analysis. Cytosolic fractions were concentrated in 3−4 times using 3 K concentrators, 20,000x*g*, 30 min, 4 °C followed by Western blot analysis. Na/K-ATPase (Cell Signaling) was used as a marker of plasma membrane fraction, and MEK-1/2 (Cell Signaling) was used as a marker of the cytosolic fraction.

2.9. Lipid droplet quantification

As previously published [44], human podocytes were fixed with 4% PFA, 2% sucrose following differentiation and/or treatment. Following fixation, cells were stained with Bodipy 493/503 (Invitrogen) and HCS Cell Mask Blue (Invitrogen) according to the manufacturer's protocols. Images were acquired using the Opera high content screening system (20x confocal lens) and the number of LDs per cell was determined using the Acapella high content image analysis software (Perkin Elmer).

2.10. Free fatty acid uptake determination

FFA uptake in immortalized podocytes isolated from Col4a3 KO mice and in collagen-treated human podocytes was measured following the manufacturer's instruction (Biovision, K408). Briefly, following serum starvation, podocytes were loaded with a fluorescent long-chain fatty acid analogue (Ex/Em=488/523, FITC-labeled fatty acids) with a proprietary nontoxic membrane-impermeable quenching agent that eliminates any fluorescence arising from the extracellular space, ensuring specific measurement of intracellular fatty acid accumulation and incubated for 1 hr at 37 °C. Fluorescence intensity was measured in a plate reader (SpectraMax M5, Molecular Devices, CA). To measure FFA uptake in GFP-DDR1b-expressing podocytes, cell lines were incubated with complete medium containing 1 μM BODIPY-C12 (558/568, red-C12, Life technologies) for 6 h. Cells were then washed three times with PBS and fixed with 4%PFA, 2% sucrose and BODIPY-C12 spot images were acquired using the Opera high content screening system (20x confocal lens) and analyzed using the Columbus high content image analysis software. Number of spots (red-C12, uptaken FFA) per cell was determined.

2.11. Cholesterol content determination

Briefly, tissue from kidney cortices and podocytes was homogenized in hypotonic buffer (10 mM HEPES pH 7.0, 15 mM KCl, 1 mM MgCl$_2$, 10 mM phosphatase inhibitors). Lipids were extracted from 100 μL of the homogenate and cholesterol content was determined using the Amplex Red Cholesterol Assay Kit (ThermoFisher Scientific, MA) following the manufacturer's instructions. Cholesteryl ester (CE) quantification was performed as previously described [62].

2.12. Triglyceride content determination

The TG content in kidney cortices and podocytes were determined using the TG Colorimetric Assay Kit (Cayman Chemical, MI) following the manufacturer's protocol. Briefly, tissue from kidney cortices was homogenized in 2 ml of diluted (1:5) standard diluent with protease inhibitors (complete Mini, Roche, Switzerland). TG standards and samples in duplicates were loaded into a 96-well plate. The reaction was initiated by adding 150 μL of diluted enzyme buffer to each well. The plate was incubated for 15 min at room temperature and fluorescence was read at 530 nm in a plate reader (SpectraMax M5, Molecular Devices, CA).

2.13. Immunoprecipitation

Plasmid containing hDDR1b (pcDNA3.1/myc-His (-) A-DR1b) was kindly provided by Dr. Rafael Fridman, Wayne State University. The hDDR1b is extended with Nhe1/EcoR1 by PCR. The PCR products were ligated into pEGFP N1 (Clontech). HEK 293 cells were co-transfected with FLAG-tagged CD36 (Sino Biological Inc) and GFP-tagged DDR1b WT plasmids. After 24 hrs, transfected HEK 293 cells were treated with ezetimibe (24 μM, 30 hrs) and immunoprecipitates of transfected HEK cell lysates were isolated using FLAG beads (Sigma-Aldrich) and the interaction between the proteins was confirmed by Western blot analysis using a GFP antibody (Clontech).

2.14. Urine samples analysis

Morning spot urine was collected bi-weekly. The urine albumin and creatinine contents were measured by ELISA and the albumin-to-creatinine ratio was determined using an assay based on the Jaffe method. The ELISA kit from Bethyl Lab (#E90−134; TX, USA) and creatinine kit from Stanbio (#0420−500; TX, USA) were used. Values are expressed as microgram albumin per milligram creatinine.

2.15. Blood sample analysis

Blood samples were analyzed for lipid panel, aspartate aminotransferase (AST), alanine transaminase (ALT) and blood urea nitrogen (BUN) in the Comparative Laboratory Core Facility of the University of Miami. Serum creatinine was determined by tandem mass spectrometry at the UAB-UCSD O'Brien Core Center (University of Alabama, Birmingham) as previously described [63].

2.16. Histology and assessment of mesangial expansion

Periodic acid-Schiff (PAS) staining of 4μm-thick tissue sections was performed using a standard protocol. Twenty glomeruli per section were analyzed for mesangial expansion by semi quantitative analysis (scale 0−4) performed by two blinded independent investigators.

2.17. Oil red O staining

Filtered Oil-Red O-Isopropanol solution (Electron Microscopy Science, PA) was diluted with water (6:4). 4 μm kidney sections were incubated with 100 μL freshly prepared Oil-Red O solution for 15 min and counterstained with Hematoxylin Harris Hg Free (VWR, PA) to detect lipid deposition. Glomerular staining was evaluated using a light microscope (Olympus BX 41, Tokyo, Japan) [64].

2.18. Picrosirius red staining

Paraffin-embedded sections (4 μm thick) were deparaffinized with xylene and a graded alcohol series. Sections were rinsed, stained for 1 h with picrosirius red in saturated aqueous picric acid, examined under a light microscope and photomicrographs were taken. Histological images were visualized using a light microscope (Olympus BX 41, Tokyo, Japan) at 40x magnification and analyzed using Image J software [65].

2.19. Transmission electron microscopy (TEM) and measurements of foot processes effacement and glomerular basement membrane thickness

For TEM, a kidney pole was fixed in 2% paraformaldehyde (PFA), 2% Glutaraldehyde in 0.1 M phosphate buffer (pH=7.4) for at least one week prior to embedding. TEM was performed as described previously [66] with minor modifications. Samples were examined with

a JEM-1011 transmission electron microscope (JEOL) at the University of Tokyo. Negatives of electron micrographs at 10,000x magnification were scanned at 600dpi. Measurements of the GBM thickness were performed using the resulting images and the Image J software. Eight images per mouse were analyzed using the distance between two points on a ruler of a photograph as a measurement scale. GBM thickness was measured in thirty different points. The number of podocyte FP along the GBM was counted manually. A FP was defined as any connected epithelial segment butting on the basement membrane, between two neighboring filtration pores or slits. From each photograph, the arithmetic mean of the foot process width (FPW) was calculated as follows: FPW = $\pi/4 * \Sigma$GBM length/Σ foot process as reported previously [67].

2.20. Statistics

Most values are presented as means with standard deviations. Some of the values that are considered non-Gaussian, are presented as median with interquartile range. Prism GraphPad 6 software was used to perform all statistical analysis. When comparing between two groups a two-tailed student's t-test or Mann-Whitney was performed, otherwise results were analyzed using one-way ANOVA or Kruskal-Wallis test. P values <0.05 were considered statistically significant.

3. Results

3.1. Phosphorylated DDR1 is increased in podocytes isolated from Col4a3KO mice and in human podocytes exposed to collagen type I

Since de novo production of Col I was described in Col4a3KO mice [27, 28], we hypothesized that DDR1 is activated by Col I in Col4a3KO mice. First, the Col I and total and phosphorylated DDR1 content in Col4a3KO mice was determined. These analyses showed increased total and phosphorylated DDR1 and Col I in kidney cortices (Figs. 1a and b) and increased alpha 1 chain of Col I in isolated glomeruli of Col4a3KO mice compared to wildtype (WT) (Fig. 1c). Furthermore,
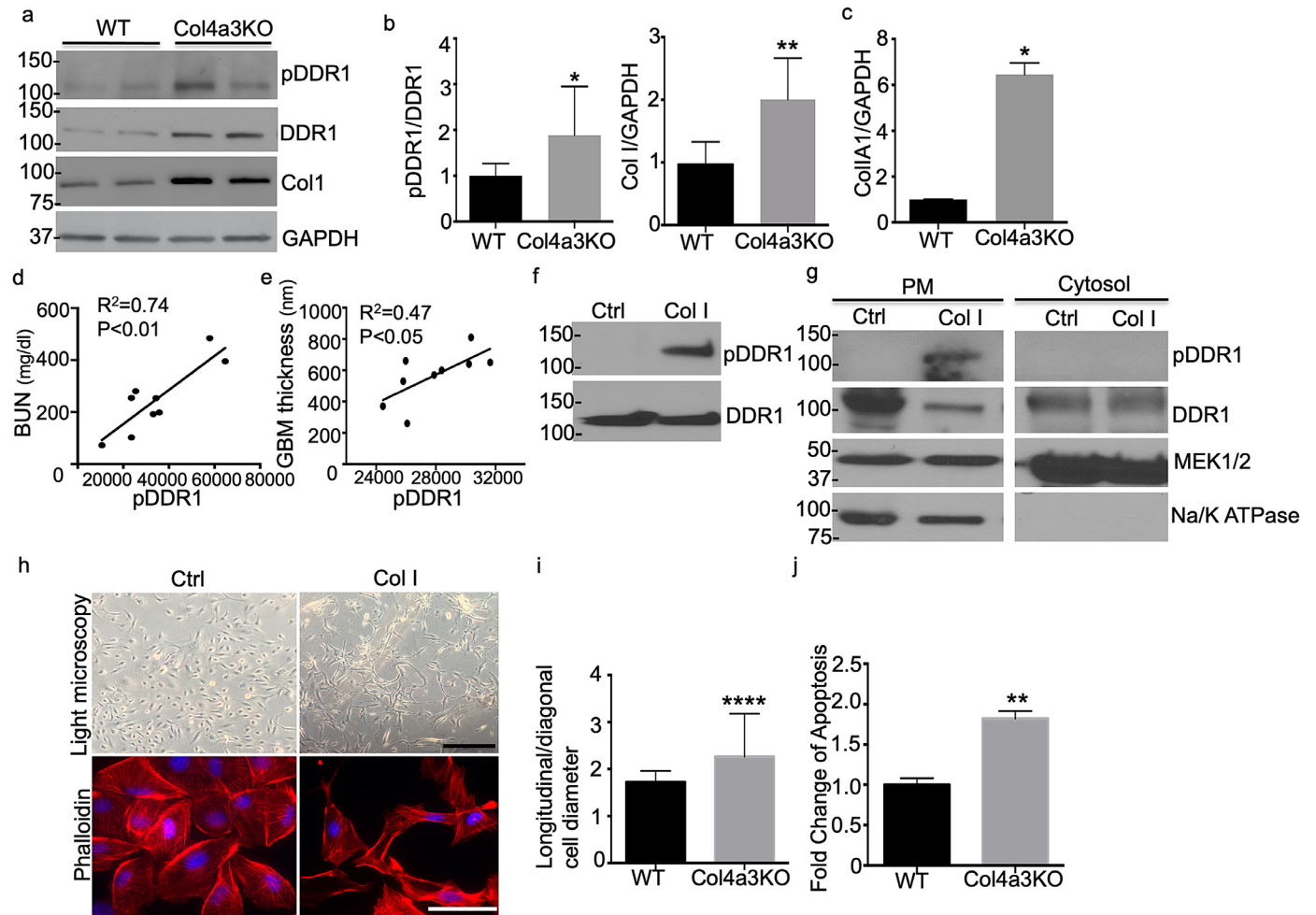
Fig. 1. pDDR1 and Col I are increased in podocytes from Col4a3 KO mice and the degree of the pDDR1 correlates with blood urea nitrogen (BUN) and with actin cytoskeleton remodeling. (a,b) DDR1 activation (pDDR1(Y513), Cell Signaling) and Col I (Aviva System) expression are increased in kidney cortices of Col4a3 KO mice as shown by pDDR1 and Col I Western blot analysis (a) and quantification of the intensity of the protein expression (b) ($N = 3–6$, *$P<0.05$ by Mann-Whitney test, **$P<0.01$ by two-tailed test). (c) mRNA expression of Col1A1 is increased in glomeruli of Col4a3 KO mice when compared to WT mice. (pooled, $N = 4–6$ per group, **$p<0.01$, by two-tailed t-test) (d) pDDR1 expression intensity levels correlate with blood urea nitrogen (BUN). ($N = 9$, *$p<0.01$, $R^2=0.74$). (e) the expression of pDDR1 correlate with the thickness of the glomerular basement membrane (GBM). ($N = 9$, *$p<0.05$, $R^2=0.47$). (f) Western blot analysis showing that DDR1 is activated by Col I in cultured human podocytes. (g) Activated DDR1 localizes primarily at the plasma membrane of podocytes. Plasma and cytosolic fractions were separated from cultured human podocytes. Western blot analysis for Na/K ATPase (plasma membrane protein) and MEK1/2 (cytosolic protein) was performed to confirm proper separation of both fractions. (h) DDR1 activation is associated with actin cytoskeleton remodeling as shown by phalloidin staining of podocytes and (i) quantification of actin remodeling. (scale bar =100 μm (upper panel) and 50 μm (lower panel), 80–100 cells were analyzed per group, ****$p<0.0001$ by Mann-Whitney test). (j) Apoptosis is increased in Col I treated podocytes when compared to untreated podocytes. ($N = 3$, **$p<0.01$ by Mann-Whitney test).

phosphorylation of DDR1b/c in Col4a3KO mice positively correlated with blood urea nitrogen (BUN) and the thickness of glomerular basement membrane (GBM), suggesting that increased activation of DDR1b/c correlates with loss of renal function (Fig. 1d) and structural changes of the GBM (Fig. 1e). Because of this positive correlation between Col I and pDDR1b/c in Col4a3KO mice (Figs. 1a and b), we hypothesized that the aberrant production of Col I in Col4a3KO mice is responsible for the enhanced activation of DDR1b/c. Interestingly, phosphorylation of DDR1b/c is significantly increased in Col I-treated human podocytes compared to untreated podocytes while total DDR1 expression levels were similar in control and Col I-treated podocytes (Fig. 1f). Cell fractionation followed by Western blot analysis demonstrates that phosphorylated DDR1b/c primarily localizes at the plasma membrane of Col I-treated podocytes (Fig. 1g). Total DDR1 levels were reduced in the plasma membranes of the Col I-treated podocytes, consistent with enhanced receptor turnover upon ligand activation. In addition, actin reorganization in Col I-treated podocytes was observed (Fig. 1h and i). This occurred in association with increased apoptosis (Fig. 1j). Taken together, these data suggest that Col I-mediated DDR1b/c activation may cause podocyte injury.

3.2. Collagen type I treated human podocytes have increased triglyceride content and free fatty acid uptake

Our previous work demonstrated that podocytes express all key proteins involved in lipid metabolism[68] and that podocyte lipotoxicity is a key determinant of podocyte injury in Col4a3KO mice and in a FSGS mouse model[42, 44]. While our previous work described an important contribution of impaired cholesterol efflux via ABCA1 to the pathogenesis of glomerular injury in AS [42], we also suggested that ABCA1 deficiency *per se* is not sufficient to cause podocyte injury [44].

More recently, it was demonstrated that dysregulated FFA metabolism also contributes to kidney disease [69]. Based on these findings, experiments were performed to elucidate how Col I induced DDR1 phosphorylation may contribute to altered FFA metabolism. Col I-treated podocytes have increased intracellular lipid droplet (LD) accumulation (Figs. 2a and b), intracellular TG content (Fig. 2c), and FFA uptake (Fig. 2d) when compared to untreated controls. Unexpectedly, levels of total and esterified cholesterol were unchanged (Figs. 2e, f and g). These data suggest that Col I-mediated DDR1 activation in podocytes contributes to increased FFA uptake and intracellular TG content in the absence of changes in cellular cholesterol content.

3.3. DDR1 activation in human podocytes causes increased triglyceride content and free fatty acid uptake

Next, we determined if DDR1 activation *per se* is sufficient to cause the increased TG content and FFA uptake and if DDR1 is responsible for Col I-induced lipid abnormalities. Human podocyte cell lines were developed expressing either GFP-tagged DDR1b wild-type (WT/DDR1b), self-activating (SA/DDR1b), kinase dead (KD/DDR1b) or empty vector (EV) (Fig. 3a) and FFA uptake and TG content was measured in these cells. SA/DDR1b-expressing podocytes displayed increased intracellular TG content (Fig. 3b) and increased FFA uptake (Fig. 3c) when compared to WT or KD/DDR1b-expressing cells. Moreover, FFA uptake and TG levels were increased in Col I-treated WT/DDR1b cells while Col I treatment of KD/DDR1b podocytes failed to increase TG levels. As expected, no significant change in cholesterol content was observed in these cells (Fig. 3d). These results suggest that activation of DDR1b in podocytes leads to increased intracellular TG content and FFA uptake.
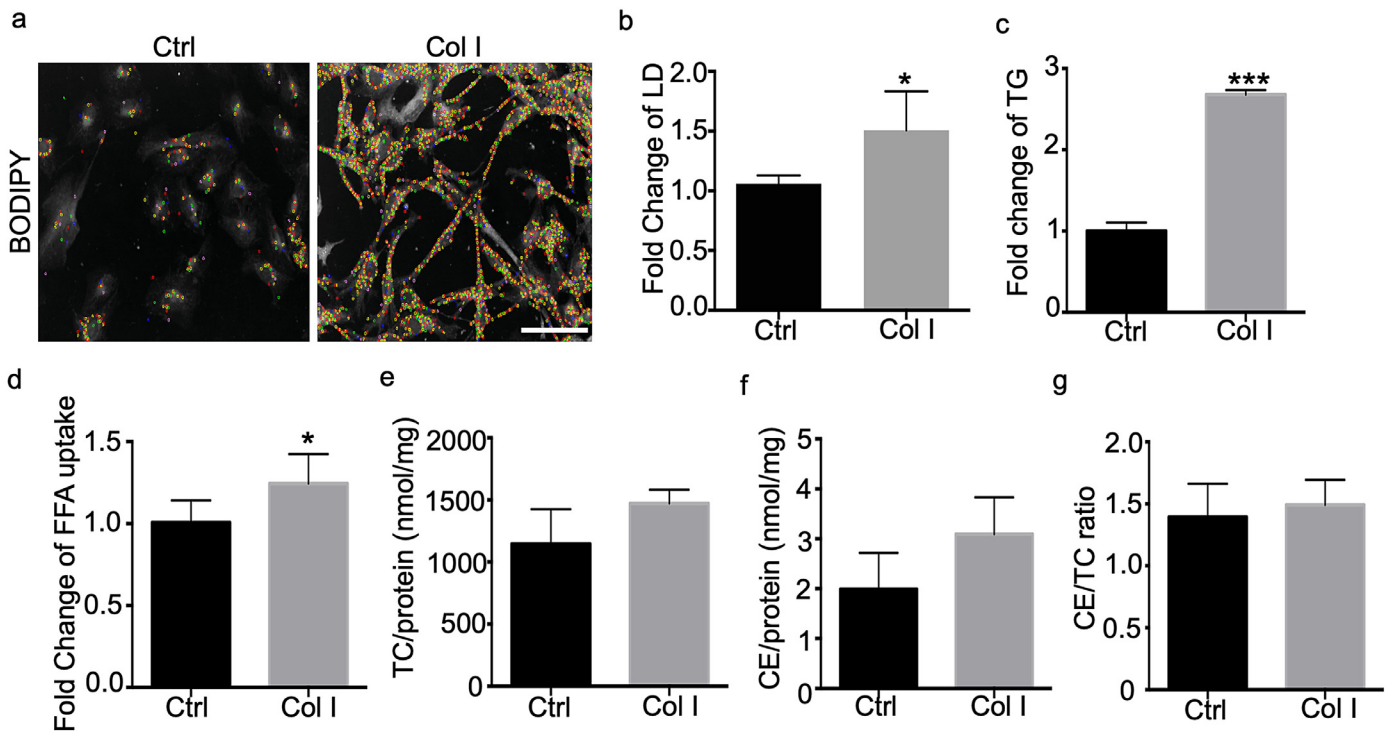
Fig. 2. Collagen treatment of human podocytes induces intracellular lipid accumulation and free fatty acid (FFA) uptake (a) Representative images of Col I treated podocytes after labeling of intracellular lipids with BODIPY. Images are taken by OPERA high content screening system and LDs were artificially colored by Acapella software program for better appreciation of single lipid droplets during the process of quantifying and visualizing the number of lipid droplets per cell (b) The number of LDs per cell was counted using the OPERA/Acapella high content screening system. Col I treated podocytes show an increased LD content (scale bar=50 μm, N = 3, *P<0.05 by two-tailed t-test.) (c) Intracellular levels of TG are increased in podocytes after Col I treatment (N = 4−6, ***P<0.001 by two-tailed t-test). (d) FFA uptake measured using fluorescent labeled FFA is increased in Col I treated podocytes (N = 3, **P<0.01 by two-tailed t-test). (e) Total intracellular cholesterol content, (f) esterified cholesterol content, (g) as well as the cholesterol ester-to-total cholesterol ratio is not significantly changed in Col I treated podocytes (N = 5 by two-tailed t-test).
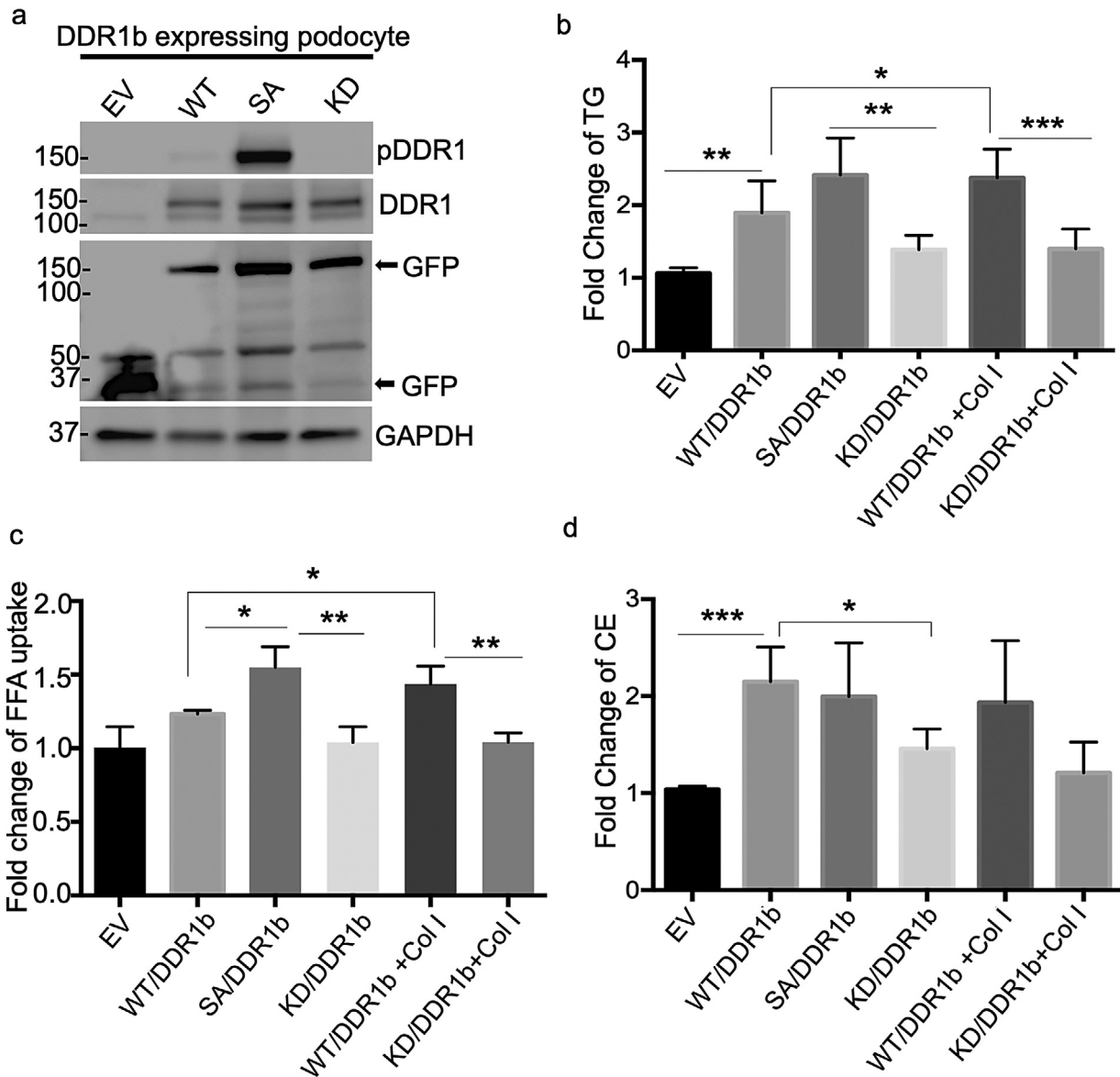
Fig. 3. DDR1b activation in human podocytes leads to increases in the triglyceride (TG) content and free fatty acid (FFA) uptake. (a) Podocyte cell lines with stable expression of GFP tagged DDR1b wild type (WT/DDR1b), self-activating (SA/DDR1b), kinase dead (KD/DDR1b) and scramble (EV) were established and protein expression was confirmed by Western blot analysis for pDDR1, DDR1, GFP and GAPDH. (b) Intracellular TG content is increased in SA/DDR1b cell line and Col I treated WT/DDR1b cell line ($N = 5$, *$P<0.05$; **$P<0.01$; ***$P<0.001$ by two-tailed t-test). (c) FFA uptake is increased in SA/DDR1b and Col I treated WT/DDR1b podocytes while no change is observed in Col I treated KD/DDR1b podocytes ($N = 3$, *$P<0.05$; **$P<0.01$ by two tailed t-test). (d) Intracellular esterified cholesterol content is increased in WT/DDR1b compared to EV podocytes and decreased in KD/DDR1b when compared to WT/DDR1b podocytes. No changes in the esterified cholesterol content are detected in SA/DDR1b or Col I treated WT/DDR1b podocytes (*$P<0.05$; ***$P<0.001$ by two tailed t-test).

3.4. DDR1b interacts with cluster of differentiation 36 (CD36), and ezetimibe reduces the interaction

Consistent with observations in podocyte cell lines expressing DDR1b, FFA uptake (Fig. 4a) and intracellular TGs (Fig. 4b) were also increased in newly developed immortalized podocytes isolated from Col4a3KO mice (AS podocytes) when compared to those isolated from WT mice (WT podocytes). CD36 is a protein involved in FFA uptake [70], cholesterol absorption [52] and activation of inflammatory pathways [50,71,72]. CD36 is expressed in tubular epithelial cells, podocytes and mesangial cells of the kidney and previous studies have shown that CD36-mediated FFA uptake induces podocyte apoptosis [49]. Therefore, expression of CD36 was measured to better understand the increased FFA uptake observed in AS podocytes. Interestingly, these analyses showed that CD36 protein levels are not significantly different between AS podocytes and WT podocytes

(Figs. 4c and d). Because CD36 levels were unchanged, it was hypothesized that DDR1 interferes with the function and/or activation of CD36 by physically interacting with the protein. To this end, co-immunoprecipitation (co-IP) experiments were performed in HEK 293 cells expressing GFP-tagged WT/DDR1b and FLAG-tagged CD36. As shown in Fig. 4e, WT/DDR1b co-immunoprecipitates with CD36, under steady state conditions. However, no binding was detected with GFP N1 (empty vector). Next, we examined whether Ezetimibe (EZ), a lipid−lowering agent, could impact DDR1b/CD36 complex formation. EZ is thought to inhibit cholesterol absorption by selectively blocking the NPC1L1 protein [73,74]; however, the exact mechanism by which EZ affects cholesterol metabolism and, more broadly, lipid metabolism remains elusive. Interestingly, studies suggest that EZ may suppress CD36 activation, as has been shown in macrophages [75] and pancreatic beta cells [56]. To test if the DDR1b/CD36 interaction could be altered by EZ, HEK 293 cells co-expressing GFP-tagged
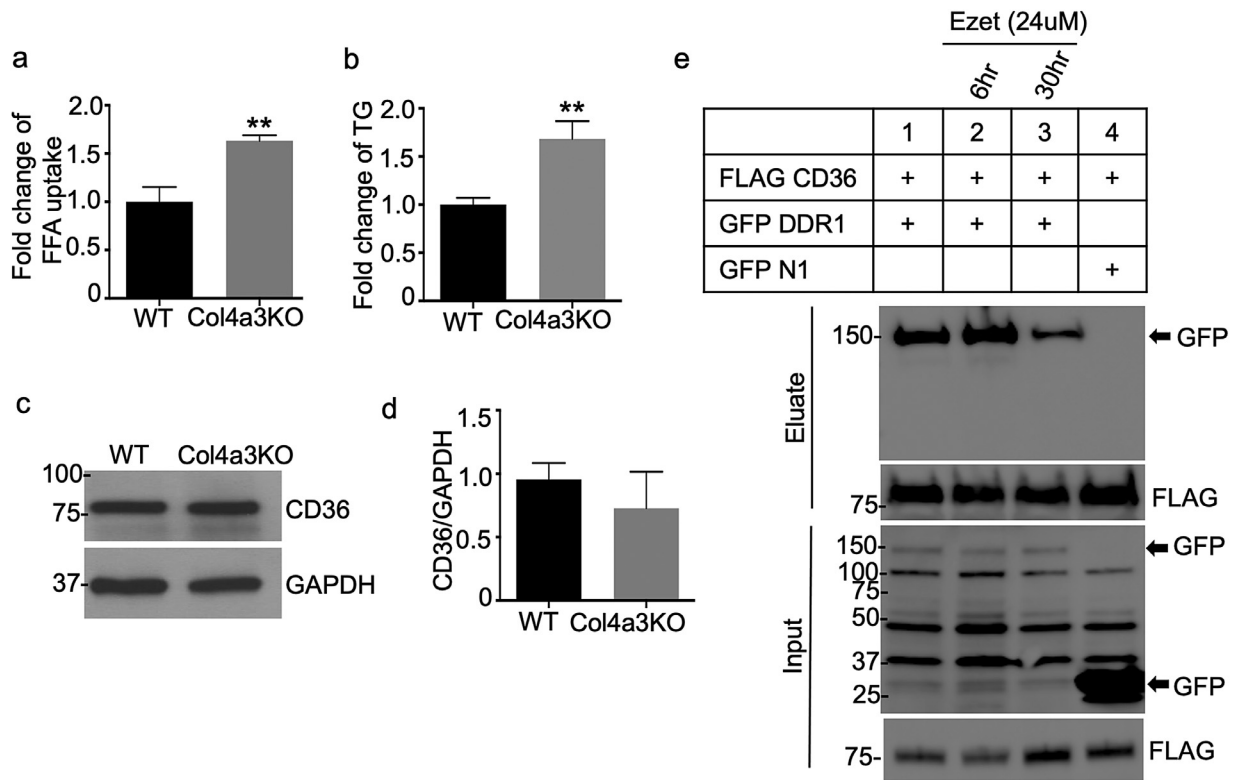
Fig. 4. Increases in the triglyceride levels and free fatty acid uptake are due to DDR1 mediated CD36 activation. (a) FFA uptake is increased in immortalized podocytes from Col4a3 KO mice ($N = 3$, **$P<0.01$ by two-tailed t-test) (b) Intracellular TG levels are increased in immortalized podocytes isolated from Col4a3 KO mice ($N = 3$, *$P<0.05$ by two-tailed t-test). (c, d) CD36 protein expression levels are unchanged in immortalized podocytes from Col4a3 KO mice ($N = 3$ by two-tailed t-test). (e) Co-immunoprecipitation analysis showing that GFP−DDR1 WT co-immunoprecipitates with FLAG-tagged CD36 in co-transfected HEK 293 cells. GFP−tagged DDR1 interacts with CD36. No binding is found with GFP N1 (control). The interaction between DDR1 and CD36 is abolished by EZ treatment (24 μM, 30 hrs).

WT/DDR1b and FLAG-tagged CD36 were treated for 6 and 30 h with EZ. Subsequent co-immunoprecipitation revealed that EZ treatment reduced the interaction between WT/DDR1b and CD36 (Fig. 4e). Taken together, these data suggest that DDR1b-mediated CD36 activation causes FFA uptake, and that EZ can block the interaction between DDR1b and CD36, suppressing CD36-mediated FFA uptake.

3.5. Ezetimibe improves renal function in a mouse model of Alport syndrome

We next investigated if EZ can preserve renal function in Col4a3KO mice. EZ was orally administered for 4 weeks at a concentration of 5 mg/kg to 4-weeks-old Col4a3KO and WT mice, at a time point when Col4a3KO mice start developing proteinuria followed by death at 8 weeks of age. Body weight (BW), albumin-to-creatinine ratio (ACR), and BUN were not different between the groups at the time of treatment initiation (Sup. Fig. 1). Mice were sacrificed at 8 weeks of age. A significant decrease in the ACR (Fig. 5a), BUN (Fig. 5b) and serum creatinine levels (Fig. 5c) was observed in Col4a3KO+EZ mice when compared to Col4a3KO mice. EZ treatment of Col4a3KO mice also significantly prevented body weight loss (Fig. 5d) and resulted in a significant reduction in mesangial expansion (Figs. 5e and f). As expected, Picrosirius red staining of kidney sections in Col4a3KO mice revealed extensive fibrosis, and EZ treatment significantly decreased fibrosis in Col4a3KO mice (Figs. 5g and h). Moreover, electron microscopy analysis revealed significant protective effects on podocyte foot process effacement and GBM thickness in Col4a3KO+EZ mice compared with Col4a3KO (Figs. 5i, j and k). These data indicate that EZ prevents renal function loss in Col4a3KO mice and suggest that the beneficial effects of EZ are due to its effect on lowering the cellular lipid content.

3.6. Ezetimibe reduces lipid accumulation by selectively preventing triglyceride accumulation in the kidney cortex from Col4a3 KO mice

To investigate whether EZ prevents lipid accumulation in the kidney cortex of Col4a3KO mice, Oil Red O (ORO) staining was performed in kidney sections from treated and untreated Col4a3KO mice. Similar to the *in vitro* studies, EZ treatment of Col4a3KO mice reduced glomerular lipid content, as determined by a decreased number of ORO positive glomeruli in EZ-treated Col4a3KO mice when compared to untreated Col4a3KO mice (Figs. 6a and b). Similarly, the renal TG content was significantly reduced in treated Col4a3KO mice when compared to untreated Col4a3KO mice (Fig. 6c), while EZ had no effect on esterified (Fig. 6d) or total renal cholesterol content (Fig. 6e). These data suggest that EZ selectively reduces the TG content in the kidney cortices of Col4a3KO mice and that this is sufficient to partially protect from renal failure.

3.7. Ezetimibe and ramipril improve renal function in Col4a3KO mice

Given that EZ proved beneficial in the treatment of renal disease in experimental AS, it was important to determine whether a combination of EZ and RM would prove superior to treatment with EZ or RM alone. Col4a3KO mice were treated with RM, EZ or with RM and EZ at 4-weeks of age for 4 weeks. A significant decrease in the ACR (Fig. 7a) and BUN (Fig. 7c) was detected in Col4a3KO mice treated with EZ, RM or with EZ + RM when compared to untreated Col4a3KO mice (Fig. 7a). While each drug alone was very effective in reducing the ACR and BUN, the combination of EZ + RM did not have a superior effect. Oral administration of EZ, RM or EZ + RM to Col4a3KO mice also resulted in a significant reduction in the serum creatinine levels
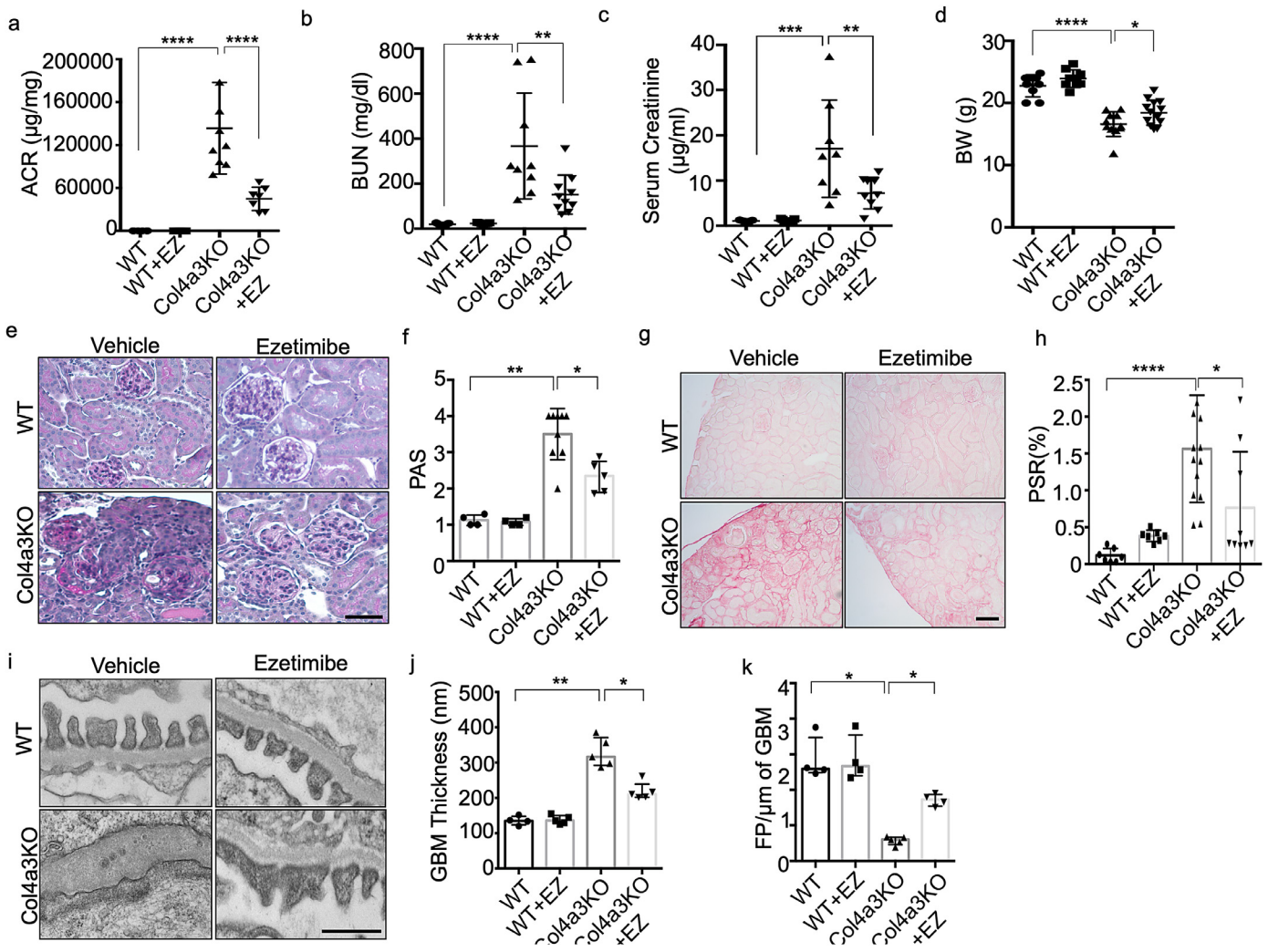
Fig. 5. Ezetimibe (EZ) improves renal function in a mouse model of Alport Syndrome. (a) Oral administration of EZ to Col4a3 KO mice results in a significant reduction in the albumin/creatinine ratio (ACR) when compared to untreated Col4a3 KO mice (n = 6−10 per group, ****p<0.0001 by one-way ANOVA followed by Tukey's multiple comparison test). (b, c) Oral administration of EZ to Col4a3 KO mice results in improvement of renal function as indicated by significantly decreased BUN (b) and serum creatinine levels (c) in EZ treated Col4a3 KO mice compared to untreated Col4a3 KO mice (N = 6−10 per group, **P<0.01, ****P<0.0001 by one-way ANOVA followed by Tukey's multiple comparison test). (d) Oral administration of EZ to Col4a3 KO mice significantly reduces the weight loss observed in Col4a3 KO mice (N = 6−10, *P<0.05, ****P<0.0001 one-way ANOVA followed by Tukey's multiple comparison test). (e, f) Oral administration of EZ to Col4a3 KO mice results in reduced mesangial expansion as demonstrated by PAS staining (e) and quantified and represented in the bar graph when compared to untreated Col4a3 KO mice (f) (scale bar=100 μm, N = 6−10 per group, *P<0.05, **P<0.001 by Kruskal-Wallis test). (g, h) Oral administration of EZ to Col4a3 KO mice results in reduced fibrosis as demonstrated by Picrosirius Red staining when compared to untreated Col4a3 KO mice (g) and quantified and represented in the bar graph (h) (scale bar=100 μm, N = 6−10 per group, *P<0.05, ****P<0.0001 by one-way ANOVA followed by Tukey's multiple comparison test). (i, j, k) Oral administration of EZ to Col4a3 KO mice results in reduced FP effacement (i) and GBM thickening (j) and an increased number of FPs per μm GBM (k) when compared to untreated Col4a3 KO mice (scale bar=500 nm, N = 3−5 per group, *P<0.05, **p<0.01 by Kruskal-Wallis test).

when compared to untreated Col4a3KO mice. While the combination of EZ + RM did not have a superior effect on the reduction of serum creatinine levels when compared to treatment with RM alone, a superior effect was observed when compared to EZ alone (Fig. 7b). Furthermore, administration of EZ, RM or EZ + RM to Col4a3KO mice also significantly prevented body weight loss during AS progression (Fig. 7d).

At sacrifice, perfused kidney sections were utilized to quantify mesangial expansion and renal fibrosis in treated and untreated Col4a3KO mice. These analyses revealed that EZ, RM and EZ + RM significantly reduced mesangial expansion (Fig. 7e) and fibrosis (Fig. 7f) in treated compared to untreated Col4a3KO mice. Bar graph quantifications for both are shown in Figs. 7g and h, respectively. These data suggest that EZ improves kidney function similar to the standard of care, RM. A non-significant trend towards a reduction in mesangial expansion and fibrosis was

observed with EZ + RM treatment, suggesting that the addition of EZ to RM may not confer further renoprotection but may be beneficial to patients intolerant to RM.

4. Discussion

The phenotypic characterization of patients with AS, where mutations in Col IV are associated with progressive renal failure, highlight the importance of the GBM composition in maintaining proper filtration [10,76,77]. Interestingly, DDR1 expression is increased in patients with renal diseases [78] and in animal models of kidney injury [79,80], while deletion of DDR1 was shown to improve renal function and fibrosis [12,78,80]. In support of these observations, inhibition of DDR1 with a small molecule compound partially prevents renal fibrosis and loss of renal function in Col4a3KO mice [29]. The present study was aimed at elucidating a novel mechanism by
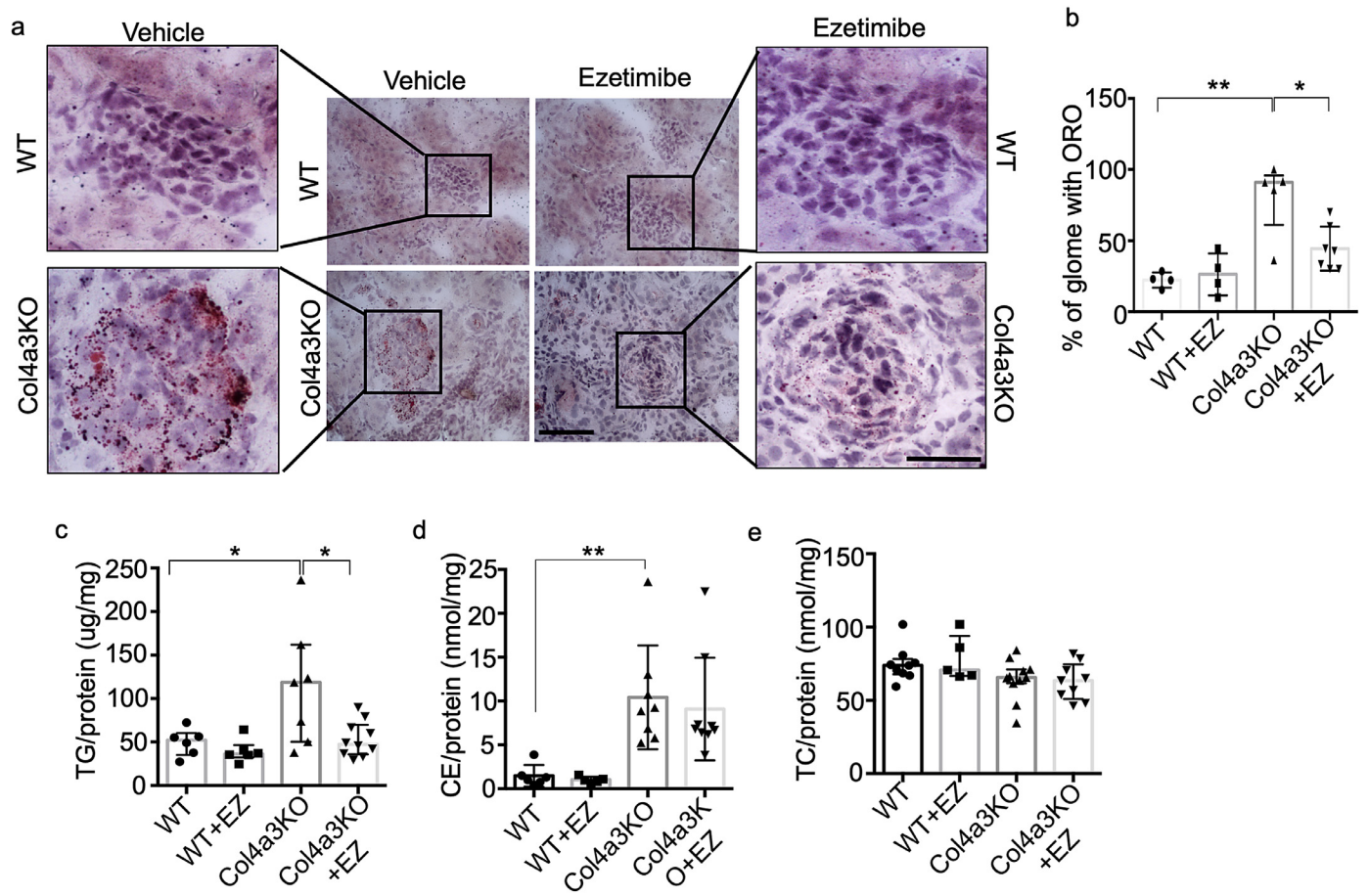
Fig. 6. Ezetimibe (EZ) reduces lipid accumulation by selectively lowering the level of triglyceride accumulation in kidney cortices of Col4a3 KO mice. (a, b) Representative image of Oil Red O (ORO) staining demonstrating that oral administration of EZ to Col4a3 KO mice results in a significant reduction in lipid accumulation when compared to untreated Col4a3 KO mice (a). Quantification of the number glomeruli with LD in ORO stained slides from 4 to 6 mice per group. The percentage of LD positive glomeruli was decreased in EZ treated Col4a3 KO mice when compared to Col4a3 KO mice (b) (scale bar=40 μm (center panel), and 50 μm (right and left panels), N = 4–6 per group, *P<0.05, **P<0.001 by Kruskal-Wallis test). (c,d,e) Oral administration of EZ results in a reduction of TG (c) but not of cholesterol levels (d, e) in kidney cortices of treated Col4a3 KO mice when compared to untreated Col4a3 KO mice (N = 6–10 per group, **P<0.01, *P<0.05 by Kruskal-Wallis test).

which aberrant DDR1 activation and podocyte lipotoxicity is caused by changes in GBM protein composition in AS, linking DDR1-dependent matrix signaling events to lipid metabolism. In addition, this work aimed at determining if treatment of Col4a3KO mice with EZ, a compound that blocks CD36 and DDR1 interaction, could improve renal function in this model.

Our findings suggest the existence of a link between DDR1-dependent signaling events and lipid metabolism. These data demonstrate that AS podocytes and kidney cortices from Col4a3KO mice have increased Col I production and pDDR1 activation, suggesting an association between increased Col I production and aberrant DDR1 activation. Data herein also show that Col I treatment of human podocytes leads to DDR1b/c activation, implying that aberrant Col I production precedes DDR1 activation. Most importantly, our data reveal that Col I treatment of human podocytes causes DDR1-dependent LD accumulation, increased CD36-mediated FFA uptake, and intracellular TG accumulation, establishing a direct link between the ECM and intracellular lipid metabolism.

While a link between DDR1 and lipid metabolism has not yet been established in renal disease, it has been shown that DDR1 deficiency in *Ldlr* knockout mice reduces atherosclerotic plaque burden [81]. In this study, expression analysis of laser-microdissected lesions revealed increased procollagen α1 (I), α3 (III) and tropoelastin expression, which is suggestive of matrix accumulation [81]. Similarly, in the kidney, DDR1 deficiency was shown to be associated

with altered GBM structure and matrix accumulation [12,78]. The observation that conditions that cause altered tissue stiffness can activate SREBP1/2, transcription factors involved in FFA and cholesterol synthesis, and cause lipid accumulation in human pluripotent stem cells [82], supports the existence of the link between matrix mediated signaling and lipid metabolism described in this study.

Lipid accumulation leading to tissue dysfunction can arise due to increased uptake or decreased lipid disposal via efflux or oxidation, and this has been reported by us in glomeruli [42] and by others in tubules [43] of Col4a3KO mice. LDs in many cell types share the same structure and are mainly comprised of TG and cholesterol esters, shielded by a phospholipid monolayer [83,84]. In keeping with our previous findings, the role of DDR1 in lipid accumulation can be explained by our novel finding of the interaction between DDR1 and CD36. This interaction supports the hypothesis that Col I induced DDR1 activation causes TG accumulation in cortices of Col4a3KO mice. This simultaneously occurs with TNF-driven reductions in ABCA1 expression and subsequent increases in renal esterified cholesterol accumulation [42,44], and both phenomena contribute to increased lipid content in Col4a3KO. This finding is consistent with others who have described an imbalance between lipid influx mediated by CD36 and efflux mediated by ABCA1 as a cause of lipid accumulation in macrophages of ulcerated carotid plaques, contributing to plaque destabilization [85]. Furthermore, a negative effect of FFA on ABCA1 and ABCG1 expression has been previously shown in
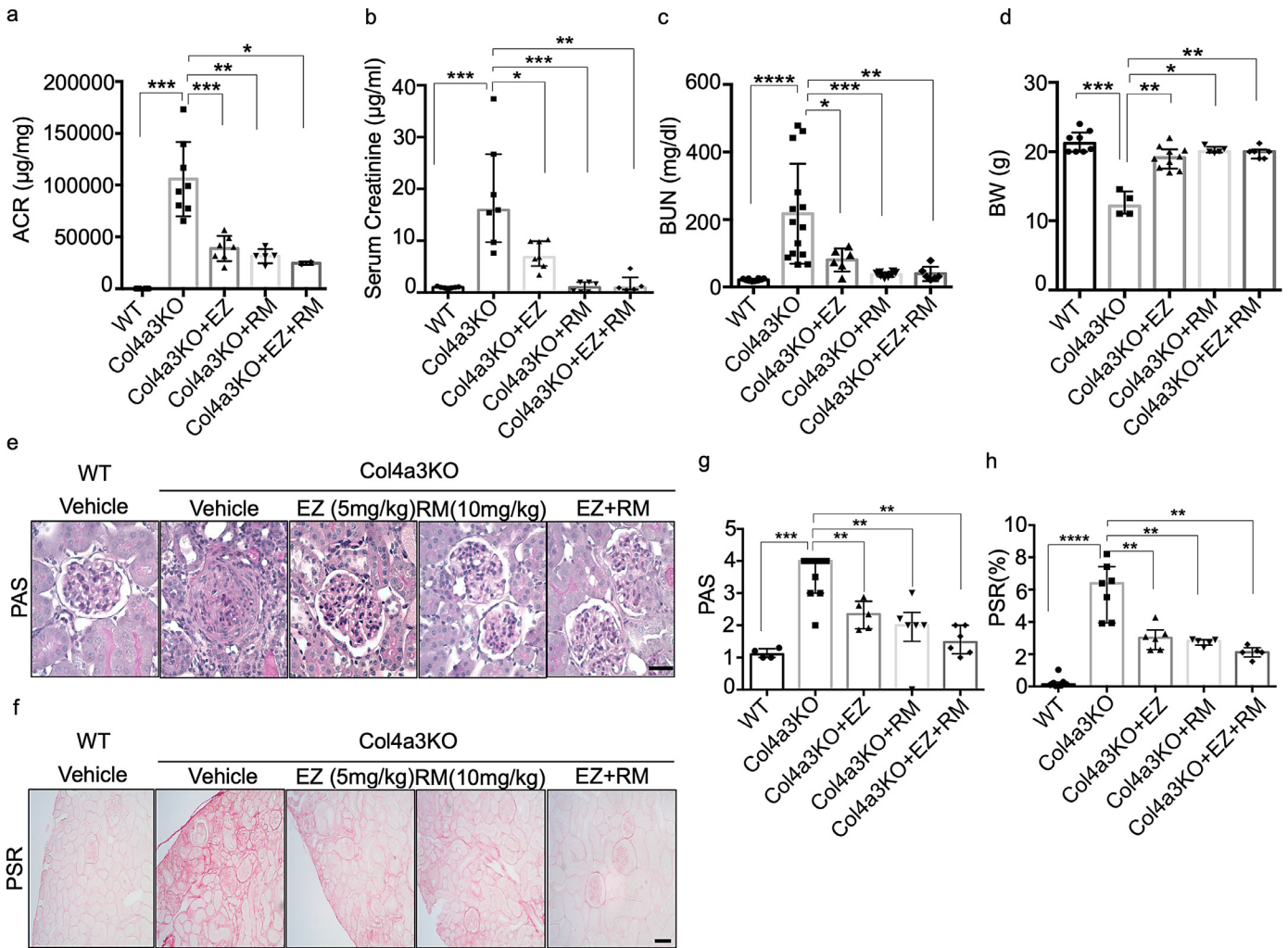
Fig. 7. Ezetimibe (EZ) and Ramipril (RM) improve renal function in Col4a3KO mice. (a) Oral administration of EZ, RM or of both drugs combined (EZ + RM) to Col4a3 KO mice results in a significant reduction in the albumin/creatinine ratio (ACR) when compared to untreated Col4a3 KO mice. The combination of EZ + RM does not have a superior effect on the reduction of the albumin/creatinine ratio when compared to EZ or RM alone (N = 5−8 per group, *P<0.05, **P<0.01, ***P<0.001 by Kruskal-Wallis test). (b) Oral administration of EZ, RM or EZ + RM to Col4a3 KO mice results in a significant reduction in the serum creatinine levels when compared to untreated Col4a3 KO mice. The combination of EZ + RM does not have a superior effect on the reduction of the serum creatinine when compared to RM alone but RM alone has a superior effect on reducing serum creatinine levels compared to EZ alone (N = 5−8 per group, *P<0.05, **P<0.01, ***P<0.001 by Kruskal-Wallis test). (c) Oral administration of EZ, RM or of EZ + RM to Col4a3 KO mice results in a significant reduction in the serum BUN levels when compared to untreated Col4a3 KO mice. The combination of EZ + RM does not have a superior effect on the reduction of the BUN levels when compared to RM alone but RM alone has a superior effect on reducing BUN levels compared to EZ alone (N = 5−8 per group, *P<0.05, **P<0.01, ***P<0.001, ****P<0.0001 by one-way ANOVA followed by Tukey's multiple comparison test). (d) Oral administration of EZ, RM or of EZ + RM to Col4a3 KO mice significantly reduces the weight loss observed in Col4a3 KO mice (N = 5−8 per group, *P<0.05, **P<0.01, ***P<0.001 by Kruskal-Wallis test). (e-h) Oral administration of EZ, RM and EZ + RM to Col4a3 KO mice results in a significant reduction in mesangial expansion and renal fibrosis when compared to untreated Col4a3-/- mice. (e) Representative image of PAS staining. (f) Representative image of Picrosirius Red staining. (g, h) Bar graph quantification of the mesangial expansion score (G) and of renal fibrosis (h) (scale bar=100 μm, N = 5−8 per group, **p<0.01, ***p<0.001, ****p<0.0001 by Kruskal-Wallis test).

macrophages [86]. Taken together, the findings in macrophages and our previous and current studies suggest that CD36 mediated increased FFA uptake affects not only TG but also esterified cholesterol accumulation by suppressing ABCA1 mRNA expression leading to increased LD accumulation in AS.

The increased FFA uptake and cytoskeletal remodeling are closely related. Inconsistent with our observation in podocyte's cytoskeletal remodeling in this study, others found that increased FFA uptake in podocytes affects changes in the cytoskeletal structure of podocytes by activating the Rho GTPases, including Rac1 and Cdc42 [87]. On the other hand, cytoskeletal remodeling is required to promote endocytosis and allow for lipid accumulation [88]. In podocytes, cofilin1 catalyzes the depolymerization of F-actin into G-actin, hence inhibiting lipid endocytosis. However, in disease conditions, impaired cofilin activity promotes F-actin formation and lipid uptake [89]. Podocyte injury in patients with obesity- related glomerulopathy can be caused

by the accumulation of lipids such as cholesterol ester and TG, which may be due to excessive endocytosis of FFA or free cholesterol [90]. These findings suggest that a positive loop pathway exists in which F-actin remodeling is associated with FFA uptake and TG accumulation in AS, and that the increased FFA causes F-actin remodeling via GTPases activity.

In support of these observations, we found that EZ blocks the interaction between DDR1 and CD36, and that EZ treatment in the Col4a3KO mice is sufficient to ameliorate the progression of AS, reduce renal LD accumulation, and decrease TG content. Unexpectedly, EZ treatment had no significant effects on cholesterol content of kidney cortices, although EZ is FDA-approved for its ability to reduce intestinal cholesterol absorption [73]. CD36 mediates the uptake of oxidized LDL (oxLDL) through binding FFA which then exposes the binding site for oxLDL on CD36 [91]. It seems possible that EZ induces conformational changes in CD36,

thus selectively opening the binding site for oxidized LDL while simultaneously blocking the binding of FFA. This could explain the mild reduction in esterified cholesterol observed in the kidneys of Col4a3KO mice treated with EZ. This conclusion is supported by previous studies in monocyte-derived macrophages showing that EZ inhibits CD36 complex assembly with its co-receptor CD13. It is also possible that EZ exercises a dose-dependent effect on cholesterol content and that an effect on kidney cholesterol content could be observed if a higher dose of EZ was used. Our data suggest that EZ significantly reduces CD36-mediated FA uptake and TG accumulation in Col4a3KO mice by reducing the DDR1-CD36 binding efficiency and subsequent CD36 activation. Whether RM may also affect renal lipid metabolism remains to be established.

In summary, this work establishes a novel mechanism by which aberrant DDR1 activation mediated changes in GBM composition causes increased FFA uptake in the kidney, contributing to increased TG accumulation and the progression of AS, or more broadly to the progression of CKD caused by mutations in Col4A3. This study also unveils a novel mechanism of DDR1-mediated kidney lipotoxicity in AS or in some patients with CKD that is amenable to therapeutic intervention by EZ. While standard of care treatment with RM improved kidney function and fibrosis as previously reported, EZ treatment results in a similar improvement of the renal phenotype of Col4a3KO mice. These data suggest that reduction of renal lipid accumulation is as effective as blockade of the renin angiotensin system in preserving kidney function in AS. Further studies investigating the clinical efficacy of EZ or of combination therapy of EZ and RM are warranted.

Author contributions

JJK and JMD conceived the project, designed the study and performed the *in vitro* and *in vivo* experiments, analyzed the data, and wrote the manuscript. SSW performed some *in vitro* experiments and most of the cell culture work. JVS, DMP, AA, XL, AM, SKM, MG and AS performed some of the *in vitro* experiments. MB, AM, HAA, and GNC help data analysis. SM and AF conceived the project, supervised the study, analyzed the data, and edited the manuscript. SSW, MP, RF and JM reviewed and edited the manuscript. All authors read and approved the final version of the manuscript. AF is the guarantor of this work and, as such, had full access to all the data in the study and takes responsibility for the integrity of the data and the accuracy of the data analysis.

Declaration of Competing Interest

A.F., and S.M. are inventors on pending or issued patents (PCT/US11/56272, PCT/US12/62594, PCT/US2019/041730, PCT/US2019/032215, PCT/US13/36484 and PCT 62/674,897) aimed to diagnosing or treating proteinuric kidney diseases. They stand to gain royalties from their future commercialization of these patents. A.F. is Vice-President of L&F Health LLC and is consultant for ZyVersa Therapeutics, Inc. ZyVersa Therapeutics, Inc has licensed worldwide rights to develop and commercialize hydroxypropyl-beta-cyclodextrin from L&F Research for the treatment of kidney disease. A.F. is founder of LipoNexT LLC. S.M. is a consultant for Kintai Therapeutics, Inc and holds equity interest in L&F Research. AF and SM are supported by Hoffman-La Roche and by Boehringer Ingelheim.

Acknowledgments

Supplementary materials

Supplementary material associated with this article can be found, in the online version, at doi:10.1016/j.ebiom.2020.103162.

References

[1] Murray CJ, Lopez AD. Measuring the global burden of disease. N Engl J Med 2013;369(5):448–57.

[2] Orth SR, Ritz E. The nephrotic syndrome. N Engl J Med 1998;338(17):1202–11.

[3] Boute N, Gribouval O, Roselli S, Benessy F, Lee H, Fuchshuber A, et al. NPHS2, encoding the glomerular protein podocin, is mutated in autosomal recessive steroid-resistant nephrotic syndrome. Nat Genet 2000;24(4):349–54.

[4] Gigante M, Pontrelli P, Montemurno E, Roca L, Aucella F, Penza R, et al. CD2AP mutations are associated with sporadic nephrotic syndrome and focal segmental glomerulosclerosis (FSGS). Nephrol Dial Transpl 2009;24(6):1858–64.

[5] Kestila M, Lenkkeri U, Mannikko M, Lamerdin J, McCready P, Putaala H, et al. Positionally cloned gene for a novel glomerular protein-nephrin-is mutated in congenital nephrotic syndrome. Mol Cell 1998;1(4):575–82.

[6] Buscher AK, Konrad M, Nagel M, Witzke O, Kribben A, Hoyer PF, et al. Mutations in podocyte genes are a rare cause of primary FSGS associated with ESRD in adult patients. Clin Nephrol 2012;78(1):47–53.

[7] Gast C, Pengelly RJ, Lyon M, Bunyan DJ, Seaby EG, Graham N, et al. Collagen (COL4A) mutations are the most frequent mutations underlying adult focal segmental glomerulosclerosis. Nephrol Dial Transpl: Off Publ Eur Dial Transpl Assoc - Eur Renal Assoc 2016;31(6):961–70.

[8] Gribouval O, Boyer O, Hummel A, Dantal J, Martinez F, Sberro-Soussan R, et al. Identification of genetic causes for sporadic steroid-resistant nephrotic syndrome in adults. Kidney Int 2018;94(5):1013–22.

[9] Groopman E, Goldstein D, Gharavi A. Diagnostic utility of exome sequencing for kidney disease. Reply. N Engl J Med 2019;380(21):2080–1.

[10] Longo I, Porcedda P, Mari F, Giachino D, Meloni I, Deplano C, et al. COL4A3/COL4A4 mutations: from familial hematuria to autosomal-dominant or recessive Alport syndrome. Kidney Int 2002;61(6):1947–56.

[11] Barker DF, Hostikka SL, Zhou J, Chow LT, Oliphant AR, Gerken SC, et al. Identification of mutations in the COL4A5 collagen gene in Alport syndrome. Science 1990;248(4960):1224–7.

[12] Gross O, Girgert R, Beirowski B, Kretzler M, Kang HG, Kruegel J, et al. Loss of collagen-receptor DDR1 delays renal fibrosis in hereditary type IV collagen disease. Matrix Biol: J Int Soc Matrix Biol 2010;29(5):346–56.

[13] Grunfeld JP. Contemporary diagnostic approach in Alport's syndrome. Ren Fail 2000;22(6):759–63.

[14] Williamson DA. Alport's syndrome of hereditary nephritis with deafness. Lancet 1961;2(7216):1321–3.

[15] Heidet L, Gubler MC. The renal lesions of Alport syndrome. J Am Soc Nephrol 2009;20(6):1210–5.

[16] Gross O, Licht C, Anders HJ, Hoppe B, Beck B, Tonshoff B, et al. Early angiotensin-converting enzyme inhibition in Alport syndrome delays renal failure and improves life expectancy. Kidney Int 2012;81(5):494–501.

[17] Gross O, Friede T, Hilgers R, Gorlitz A, Gavenis K, Ahmed R, et al. Safety and efficacy of the ACE-inhibitor ramipril in Alport syndrome: the double-blind, randomized, placebo-controlled, multicenter phase III EARLY PRO-TECT Alport trial in pediatric patients. ISRN Pediatr 2012;2012:436046.

[18] Khoshnoodi J, Pedchenko V, Hudson BG. Mammalian collagen IV. Microsc Res Tech 2008;71(5):357–70.

[19] Hudson BG. The molecular basis of Goodpasture and Alport syndromes: beacons for the discovery of the collagen IV family. J Am Soc Nephrol 2004;15(10):2514–27.

[20] Hudson BG, Tryggvason K, Sundaramoorthy M, Neilson EG. Alport's syndrome, Goodpasture's syndrome, and type IV collagen. N Engl J Med 2003;348(25):2543–56.

[21] Miner JH, Baigent C, Flinter F, Gross O, Judge P, Kashtan CE, et al. The 2014 international workshop on Alport syndrome. Kidney Int 2014;86(4):679–84.

[22] Abrahamson DR, Hudson BG, Stroganova L, Borza DB, St John PL. Cellular origins of type IV collagen networks in developing glomeruli. J Am Soc Nephrol 2009;20(7):1471–9.

[23] Heidet L, Cai Y, Guicharnaud L, Antignac C, Gubler MC. Glomerular expression of type IV collagen chains in normal and X-linked Alport syndrome kidneys. Am J Pathol 2000;156(6):1901–10.

[24] Kashtan CE, Kim Y. Distribution of the alpha 1 and alpha 2 chains of collagen IV and of collagens V and VI in Alport syndrome. Kidney Int 1992;42(1):115–26.

[25] Kashtan CE. Alport syndrome. Kidney Int Suppl 1997;58:S69–71.

[26] Kalluri R, Shield CF, Todd P, Hudson BG, Neilson EG. Isoform switching of type IV collagen is developmentally arrested in X-linked Alport syndrome leading to

increased susceptibility of renal basement membranes to endoproteolysis. J Clin Invest 1997;99(10):2470–8.

[27] Muckova P, Wendler S, Rubel D, Buchler R, Alert M, Gross O, et al. Preclinical alterations in the serum of COL(IV)A3(-)/(-) mice as early biomarkers of Alport syndrome. J Proteome Res 2015;14(12):5202–14.

[28] Lennon R, Byron A, Humphries JD, Randles MJ, Carisey A, Murphy S, et al. Global analysis reveals the complexity of the human glomerular extracellular matrix. J Am Soc Nephrol 2014;25(5):939–51.

[29] Richter H, Satz AL, Bedoucha M, Buettelmann B, Petersen AC, Harmeier A, et al. DNA-encoded library-derived DDR1 inhibitor prevents fibrosis and renal function loss in a genetic mouse model of Alport syndrome. ACS Chem Biol 2019;14 (1):37–49.

[30] Faul C, Asanuma K, Yanagida-Asanuma E, Kim K, Mundel P. Actin up: regulation of podocyte structure and function by components of the actin cytoskeleton. Trends Cell Biol 2007;17(9):428–37.

[31] Mundel P, Proteinuria Reiser J. An enzymatic disease of the podocyte? Kidney Int 2010;77(7):571–80.

[32] Lennon R, Randles MJ, Humphries MJ. The importance of podocyte adhesion for a healthy glomerulus. Front Endocrinol (Lausanne) 2014;5:160.

[33] Byron A, Randles MJ, Humphries JD, Mironov A, Hamidi H, Harris S, et al. Glomerular cell cross-talk influences composition and assembly of extracellular matrix. J Am Soc Nephrol 2014;25(5):953–66.

[34] Pozzi A, Jarad G, Moeckel GW, Coffa S, Zhang X, Gewin L, et al. Beta1 integrin expression by podocytes is required to maintain glomerular structural integrity. Dev Biol 2008;316(2):288–301.

[35] Hynes RO. Integrins: bidirectional, allosteric signaling machines. Cell 2002;110 (6):673–87.

[36] Kadler KE, Baldock C, Bella J, Boot-Handford RP. Collagens at a glance. J Cell Sci 2007;120(Pt 12):1955–8.

[37] Vogel W, Gish GD, Alves F, Pawson T. The discoidin domain receptor tyrosine kinases are activated by collagen. Mol Cell 1997;1(1):13–23.

[38] Leitinger B. Discoidin domain receptor functions in physiological and pathological conditions. Int Rev Cell Mol Biol 2014;310:39–87.

[39] Curat CA, Vogel WF. Discoidin domain receptor 1 controls growth and adhesion of mesangial cells. J Am Soc Nephrol 2002;13(11):2648–56.

[40] Abdulhussein R, McFadden C, Fuentes-Prior P, Vogel WF. Exploring the collagen-binding site of the DDR1 tyrosine kinase receptor. J Biol Chem 2004;279 (30):31462–70.

[41] Borza CM, Pozzi A. Discoidin domain receptors in disease. Matrix Biol 2014;34:185–92.

[42] Mitrofanova A, Molina J, Varona Santos J, Guzman J, Morales XA, Ducasa GM, et al. Hydroxypropyl-beta-cyclodextrin protects from kidney disease in experimental Alport syndrome and focal segmental glomerulosclerosis. Kidney Int 2018;94 (6):1151–9.

[43] Ding W, Yousefi K, Goncalves S, Goldstein BJ, Sabater AL, Kloosterboer A, et al. Osteopontin deficiency ameliorates Alport pathology by preventing tubular metabolic deficits. JCI Insight 2018;3(6).

[44] Pedigo CE, Ducasa GM, Leclercq F, Sloan A, Mitrofanova A, Hashmi T, et al. Local TNF causes NFATc1-dependent cholesterol-mediated podocyte injury. J Clin Invest 2016;126(9):3336–50.

[45] Herman-Edelstein M, Scherzer P, Tobar A, Levi M, Gafter U. Altered renal lipid metabolism and renal lipid accumulation in human diabetic nephropathy. J Lipid Res 2014;55(3):561–72.

[46] Merscher-Gomez S, Guzman J, Pedigo CE, Lehto M, Aguillon-Prada R, Mendez A, et al. Cyclodextrin protects podocytes in diabetic kidney disease. Diabetes 2013;62(11):3817–27.

[47] Wang Z, Jiang T, Li J, Proctor G, McManaman JL, Lucia S, et al. Regulation of renal lipid metabolism, lipid accumulation, and glomerulosclerosis in FVBdb/db mice with type 2 diabetes. Diabetes 2005;54(8):2328–35.

[48] Sieber J, Jehle AW. Free Fatty acids and their metabolism affect function and survival of podocytes. Front Endocrinol (Lausanne) 2014;5:186.

[49] Hua W, Huang HZ, Tan LT, Wan JM, Gui HB, Zhao L, et al. CD36 mediated fatty acid-induced podocyte apoptosis via oxidative stress. PLoS ONE 2015;10(5): e0127507.

[50] Febbraio M, Hajjar DP, Silverstein RL. CD36: a class B scavenger receptor involved in angiogenesis, atherosclerosis, inflammation, and lipid metabolism. J Clin Invest 2001;108(6):785–91.

[51] Han J, Hajjar DP, Febbraio M, Nicholson AC. Native and modified low density lipoproteins increase the functional expression of the macrophage class B scavenger receptor, CD36. J Biol Chem 1997;272(34):21654–9.

[52] Nassir F, Wilson B, Han X, Gross RW, Abumrad NA. CD36 is important for fatty acid and cholesterol uptake by the proximal but not distal intestine. J Biol Chem 2007;282(27):19493–501.

[53] Hajri T, Han XX, Bonen A, Abumrad NA. Defective fatty acid uptake modulates insulin responsiveness and metabolic responses to diet in CD36-null mice. J Clin Invest 2002;109(10):1381–9.

[54] During A, Dawson HD, Harrison EH. Carotenoid transport is decreased and expression of the lipid transporters SR-BI, NPC1L1, and ABCA1 is downregulated in Caco-2 cells treated with ezetimibe. J Nutr 2005;135(10):2305–12.

[55] Qin L, Yang YB, Yang YX, Zhu N, Liu Z, Ni YG, et al. Inhibition of macrophage-derived foam cell formation by ezetimibe via the caveolin-1/MAPK pathway. Clin Exp Pharmacol Physiol 2016;43(2):182–92.

[56] Yoon JS, Moon JS, Kim YW, Won KC, Lee HW. The Glucotoxicity Protecting Effect of Ezetimibe in Pancreatic Beta Cells via Inhibition of CD36. J Korean Med Sci 2016;31(4):547–52.

[57] Jat PS, Noble MD, Ataliotis P, Tanaka Y, Yannoutsos N, Larsen L, et al. Direct derivation of conditionally immortal cell lines from an H-2Kb-tsA58 transgenic mouse. Proc Natl Acad Sci U S A 1991;88(12):5096–100.

[58] Mundel P, Reiser J, Zuniga Mejia Borja A, Pavenstadt H, Davidson GR, Kriz W, et al. Rearrangements of the cytoskeleton and cell contacts induce process formation during differentiation of conditionally immortalized mouse podocyte cell lines. Exp Cell Res 1997;236(1):248–58.

[59] Fu HL, Valiathan RR, Payne L, Kumarasiri M, Mahasenan KV, Mobashery S, et al. Glycosylation at Asn211 regulates the activation state of the discoidin domain receptor 1 (DDR1). J Biol Chem 2014;289(13):9275–87.

[60] Vogel W, Brakebusch C, Fassler R, Alves F, Ruggiero F, Pawson T. Discoidin domain receptor 1 is activated independently of beta(1) integrin. J Biol Chem 2000;275 (8):5779–84.

[61] Saleem MA, O'Hare MJ, Reiser J, Coward RJ, Inward CD, Farren T, et al. A conditionally immortalized human podocyte cell line demonstrating nephrin and podocin expression. J Am Soc Nephrol 2002;13(3):630–8.

[62] Mizoguchi T, Edano T, Koshi T. A method of direct measurement for the enzymatic determination of cholesteryl esters. J Lipid Res 2004;45(2):396–401.

[63] Takahashi N, Boysen G, Li F, Li Y, Swenberg JA. Tandem mass spectrometry measurements of creatinine in mouse plasma and urine for determining glomerular filtration rate. Kidney Int 2007;71(3):266–71.

[64] Mehlem A, Hagberg CE, Muhl L, Eriksson U, Falkevall A. Imaging of neutral lipids by oil red O for analyzing the metabolic status in health and disease. Nat Protoc 2013;8(6):1149–54.

[65] Ioannou GN, Haigh WG, Thorning D, Savard C. Hepatic cholesterol crystals and crown-like structures distinguish NASH from simple steatosis. J Lipid Res 2013;54(5):1326–34.

[66] Choudhary V, Ojha N, Golden A, Prinz WA. A conserved family of proteins facilitates nascent lipid droplet budding from the ER. J Cell Biol 2015;211 (2):261–71.

[67] van den Berg JG, van den Bergh Weerman MA, Assmann KJ, Weening JJ, Florquin S. Podocyte foot process effacement is not correlated with the level of proteinuria in human glomerulopathies. Kidney Int 2004;66(5):1901–6.

[68] Fornoni A, Merscher S, Kopp JB. Lipid biology of the podocyte−new perspectives offer new opportunities. Nat Rev Nephrol 2014;10(7):379–88.

[69] Kang HM, Ahn SH, Choi P, Ko YA, Han SH, Chinga F, et al. Defective fatty acid oxidation in renal tubular epithelial cells has a key role in kidney fibrosis development. Nat Med 2015;21(1):37–46.

[70] Xu S, Jay A, Brunaldi K, Huang N, Hamilton JA. CD36 enhances fatty acid uptake by increasing the rate of intracellular esterification but not transport across the plasma membrane. Biochemistry 2013;52(41):7254–61.

[71] Endemann G, Stanton LW, Madden KS, Bryant CM, White RT, Protter AA. CD36 is a receptor for oxidized low density lipoprotein. J Biol Chem 1993;268(16):11811–6.

[72] Stewart CR, Stuart LM, Wilkinson K, van Gils JM, Deng J, Halle A, et al. CD36 ligands promote sterile inflammation through assembly of a Toll-like receptor 4 and 6 heterodimer. Nat Immunol 2010;11(2):155–61.

[73] Chang TY, Chang C. Ezetimibe blocks internalization of the NPC1L1/cholesterol complex. Cell Metab 2008;7(6):469–71.

[74] Altmann SW, Davis Jr. HR, Zhu LJ, Yao X, Hoos LM, Tetzloff G, et al. Niemann-Pick C1 Like 1 protein is critical for intestinal cholesterol absorption. Science 2004;303 (5661):1201–4.

[75] Orso E, Werner T, Wolf Z, Bandulik S, Kramer W, Schmitz G. Ezetimib influences the expression of raft-associated antigens in human monocytes. Cytometry A 2006;69(3):206–8.

[76] Hudson BG, Reeders ST, Tryggvason K. Type IV collagen: structure, gene organization, and role in human diseases. Molecular basis of Goodpasture and Alport syndromes and diffuse leiomyomatosis. J Biol Chem 1993;268(35):26033–6.

[77] Nagel M, Nagorka S, Gross O. Novel COL4A5, COL4A4, and COL4A3 mutations in Alport syndrome. Hum Mutat 2005;26(1):60.

[78] Kerroch M, Guerrot D, Vandermeersch S, Placier S, Mesnard L, Jouanneau C, et al. Genetic inhibition of discoidin domain receptor 1 protects mice against crescentic glomerulonephritis. FASEB J 2012;26(10):4079–91.

[79] Kerroch M, Alfieri C, Dorison A, Boffa JJ, Chatziantoniou C, Dussaule JC. Protective effects of genetic inhibition of discoidin domain receptor 1 in experimental renal disease. Sci Rep 2016;6:21262.

[80] Guerrot D, Kerroch M, Placier S, Vandermeersch S, Trivin C, Mael-Ainin M, et al. Discoidin domain receptor 1 is a major mediator of inflammation and fibrosis in obstructive nephropathy. Am J Pathol 2011;179(1):83–91.

[81] Franco C, Hou G, Ahmad PJ, Fu EY, Koh L, Vogel WF, et al. Discoidin domain receptor 1 (ddr1) deletion decreases atherosclerosis by accelerating matrix accumulation and reducing inflammation in low-density lipoprotein receptor-deficient mice. Circ Res 2008;102(10):1202–11.

[82] Romani P, Brian I, Santinon G, Pocaterra A, Audano M, Pedretti S, et al. Extracellular matrix mechanical cues regulate lipid metabolism through Lipin-1 and SREBP. Nat Cell Biol 2019;21(3):338–47.

[83] Czabany T, Wagner A, Zweytick D, Lohner K, Leitner E, Ingolic E, et al. Structural and biochemical properties of lipid particles from the yeast Saccharomyces cerevisiae. J Biol Chem 2008;283(25):17065–74.

[84] Cheng J, Fujita A, Ohsaki Y, Suzuki M, Shinohara Y, Fujimoto T. Quantitative electron microscopy shows uniform incorporation of triglycerides into existing lipid droplets. Histochem Cell Biol 2009;132(3):281–91.

[85] Isoviita PM, Nuotio K, Saksi J, Turunen R, Ijas P, Pitkaniemi J, et al. An imbalance between CD36 and ABCA1 protein expression favors lipid accumulation in stroke-prone ulcerated carotid plaques. Stroke 2010;41(2):389–93.

[86] Uehara Y, Miura S, von Eckardstein A, Abe S, Fujii A, Matsuo Y, et al. Unsaturated fatty acids suppress the expression of the ATP-binding cassette transporter G1 (ABCG1) and ABCA1 genes via an LXR/RXR responsive element. Atherosclerosis 2007;191(1):11–21.

[87] Chung JJ, Huber TB, Godel M, Jarad G, Hartleben B, Kwoh C, et al. Albumin-associated free fatty acids induce macropinocytosis in podocytes. J Clin Invest 2015;125 (6):2307–16.

[88] Bamburg JR. Proteins of the ADF/cofilin family: essential regulators of actin dynamics. Annu Rev Cell Dev Biol 1999;15:185–230.

[89] Ashworth S, Teng B, Kaufeld J, Miller E, Tossidou I, Englert C, et al. Cofilin-1 inactivation leads to proteinuria-studies in zebrafish, mice and humans. PLoS ONE 2010;5(9):e12626.

[90] Shi Y, Wang C, Zhou X, Li Y, Ma Y, Zhang R, et al. Downregulation of PTEN promotes podocyte endocytosis of lipids aggravating obesity-related glomerulopathy. Am J Physiol Renal Physiol 2020;318(3):F589–F99.

[91] Jay AG, Chen AN, Paz MA, Hung JP, Hamilton JA. CD36 binds oxidized low density lipoprotein (LDL) in a mechanism dependent upon fatty acid binding. J Biol Chem 2015;290(8):4590–603.